Conformation of Star Polymers in High Molecular Weight Solvents

E. Raphaël,*,†,‡,§ P. Pincus,§,∥ and G. H. Fredrickson§,⊥

Institute for Polymer & Organic Solids and Departments of Materials, Physics, and Chemical and Nuclear Engineering, University of California, Santa Barbara, California 93106

Received August 28, 1992; Revised Manuscript Received January 12, 1993

ABSTRACT: Ten years ago Daoud and Cotton proposed a very elegant model for the static properties of an isolated star-shaped polymer in a solvent of low molecular weight. Here we investigate the static behavior of a star-shaped polymer (f arms; N monomers per arm) dissolved in a melt of linear chains (with degree of polymerization $P < N$), chemically identical to the star arms. We predict that the N-monomer volume fraction varies as $\phi_N(r) \cong 1$ (meltlike region) for $r < af^{1/2}P^{1/4}$ and $\phi_N(r) \cong (r/a)^{-4/3}f^{2/3}P^{1/3}$ for $r > af^{1/2}P^{1/4}$. We briefly discuss concentration effects. In addition to this analysis, we also review and discuss some of the properties of polymer chains tethered by one end to a flat solid surface. Our whole study is restricted to scaling laws; the exact prefactors in all our formulas remain undetermined.

1. Introduction

In recent years there has been an increased interest in star-shaped polymers.[1-18] A particularly simple model for the static properties of an isolated star-shaped polymer in a solvent of low molecular weight was proposed by Daoud and Cotton (DC) 10 years ago.[1] Consider a star-shaped polymer made of f identical arms. Each arm consists of N monomers of size a. The solvent quality is described by an excluded-volume parameter v which, by assumption, satisfies $0 < v \leq a^3$ ("good solvent"); the terminology used throughout this paper to describe the solvent quality is explained in Appendix 1. Since the volume accessible to a given chain increases with the distance from the center of the star, r, one expects the monomer volume fraction, ϕ, to be a decreasing function of r. According to DC, each arm can be seen as a succession of growing spherical "blobs" (see Figure 1). Within one blob the arm behaves as an isolated chain. At a given distance r from the center, there are f blobs, one for each polymer chain. Since f blobs cover a sphere of radius r, the blob radius is given by

$$\xi(r) \cong rf^{-1/2} \tag{1.1}$$

According to eq A1.6 of Appendix 1, the number $n(r)$ of monomers per blob of size $\xi(r)$ is given by

$$\xi(r) \cong an(r)^{3/5}(v/a^3)^{1/5} \tag{1.2}$$

Combining eqs 1.1 and 1.2, we obtain for the monomer volume fraction

$$\phi(r) \cong n(r)/\xi^3(r) \cong (r/a)^{-4/3}f^{2/3}(v/a^3)^{-1/3} \tag{1.3}$$

Equation 1.2 explicitly assumes that the blob size $\xi(r) \cong rf^{-1/2}$ is larger than the size of a *thermal* blob $l_c \cong a(v/a^3)^{-1}$ introduced in Appendix 1 (see Figure 1). Therefore, eqs 1.2 and 1.3 are valid only in the outer part of the star. This region is defined by $r \geq r_1$ with

$$r_1 \cong af^{1/2}(v/a^3)^{-1} \tag{1.4}$$

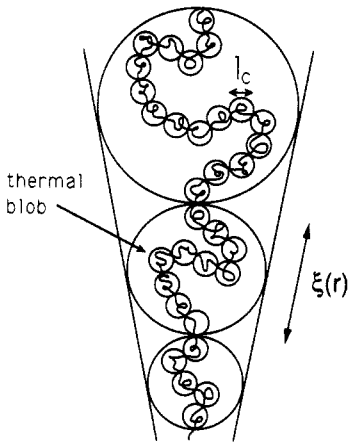

Figure 1. Daoud-Cotton conception of the outer region ($r > r_1$) of a star polymer dissolved in a good solvent of low molecular weight. In this outer region the blob size $\xi(r) \cong rf^{-1/2}$ is greater than thermal blob size $l_c \cong a(v/a^3)^{-1}$.

For distances smaller than r_1, DC assume that each arm can be pictured as a succession of growing *ideal spherical* blobs. (We will see that this assumption is indeed correct, provided one takes three-body interactions into account.) From geometric considerations, the blob size, $\xi(r)$, is still given by eq 1.1 but eq 1.2 should be replaced by

$$\xi(r) \cong an(r)^{1/2} \tag{1.5}$$

since now, within one blob, the arm behaves like an ideal chain.

Thus, for $r \leq r_1$, the monomer volume fraction is given by (see eqs 1.1 and 1.5)

$$\phi(r) \cong n(r)/\xi^3(r) \cong (r/a)^{-1}f^{1/2} \tag{1.6}$$

At still smaller distances to the center of the star, one reaches a distance r_2 below which the monomer volume fraction is unity ($\phi \cong 1$). From eq 1.6 we get

$$r_2 \cong af^{1/2} \tag{1.7}$$

Therefore, according to the DC model, a star with long enough arms consists of three regions: (1) an inner meltlike region ($r \ll r_2$), (2) an intermediate region ($r_2 \ll r \ll r_1$) where the blobs are ideal, and (3) an outer region ($r_1 \ll r \ll R$) where the blobs are swollen. In these three regions

† On leave from Laboratoire de la Matière Condensée, Collège de France, 75231 Paris Cedex 05, France.
‡ Institute for Polymer & Organic Solids.
§ Department of Materials.
∥ Department of Physics.
⊥ Department of Chemical and Nuclear Engineering.

0024-9297/93/2226-1996$04.00/0

the monomer volume fraction is respectively given by

$$\phi(r) \cong 1 \qquad r < af^{1/2} \tag{1.8a}$$

$$\phi(r) \cong (r/a)^{-1}f^{1/2} \qquad af^{1/2} < r < af^{1/2}(v/a^3)^{-1} \tag{1.8b}$$

$$\phi(r) \cong (r/a)^{-4/3}f^{2/3}(v/a^3)^{-1/3} \qquad af^{1/2}(v/a^3)^{-1} < r < R \tag{1.8c}$$

Note that in the limiting case of an athermal solvent ($v = a^3$) the intermediate region disappears ($r_1 \cong r_2$).

The radius of the star, R, can be deduced from the condition

$$Nfa^3 = \int_0^R d^3r\, \phi(r) \tag{1.9}$$

Using eq 1.8, we obtain

$$R \cong aN^{3/5}f^{1/5}(v/a^3)^{1/5} \qquad N \gg f^{1/2}(v/a^3)^{-2} \tag{1.10a}$$

$$R \cong aN^{1/2}f^{1/4} \qquad f^{1/2}(v/a^3)^{-2} \gg N \gg f^{1/2} \tag{1.10b}$$

$$R \cong aN^{1/3}f^{1/3} \qquad f^{1/2} \gg N \tag{1.10c}$$

The results (1.10a–c) for the star radius can also be obtained from a simple Flory-type free energy, as explained in Appendix 5.

The scaling relations $\phi(r) \propto (r/a)^{-4/3}f^{2/3}$ and $R \propto aN^{3/5}f^{1/5}$ describing the outer region of the star have been well confirmed by the molecular dynamics simulations of Grest et al.[9,12] There is also a good agreement between the scaling prediction $R \propto aN^{3/5}f^{1/5}$ and the experimental data of Khasat et al.[10] However, the crossover between the outer and the intermediate regions has (to the best of our knowledge) not yet been observed.[14] This might be due to the fact that $r_1 \cong af^{1/2}(v/a^3)^{-1}$ is usually rather small and close to r_2 ($r_1/r_2 \cong (v/a^3)^{-1}$), unless one investigates stars with many arms in the immediate vicinity of the Θ point.

In order to observe the intermediate region predicted by DC, one might consider replacing the low molecular weight solvent by a melt of linear chains, with degree of polymerization $P < N$, chemically identical to the star arms. Indeed, as explained at the end of Appendix 2, there exists an well-known analogy between (a) the behavior of an isolated linear chain (N monomers) dissolved in a good solvent ($0 < v \leq a^3$) of low molecular weight and (b) the behavior of an isolated linear chain (N monomers) dissolved in a melt of shorter (P monomers, with $P < N$), chemically identical chains.

One moves from one case to another by simply using the substitution

$$(v/a^3)^{-1} \leftrightarrow P \tag{1.11}$$

Consequently, in the case of a star polymer (f arms, N monomers per arm), immersed in a melt of linear, chemically identical chains (P monomers, with $P < N$), one might expect the monomer volume fraction to be given by (see eqs 1.8 and 1.11)

$$\phi(r) \cong 1 \qquad r < af^{1/2} \tag{1.12a}$$

$$\phi(r) \cong (r/a)^{-1}f^{1/2} \qquad af^{1/2} < r < af^{1/2}P \tag{1.12b}$$

$$\phi(r) \cong (r/a)^{-4/3}f^{2/3}P^{1/3} \qquad af^{1/2}P < r < R \tag{1.12c}$$

and the star radius by (see eqs 1.10 and 1.11)

$$R \cong aN^{3/5}f^{1/5}P^{-1/5} \qquad N \gg f^{1/2}P^2 \tag{1.13a}$$

$$R \cong aN^{1/2}f^{1/4} \qquad f^{1/2}P^2 \gg N \gg f^{1/2} \tag{1.13b}$$

$$R \cong aN^{1/3}f^{1/3} \qquad f^{1/2} \gg N \tag{1.13c}$$

According to eqs 1.12 and 1.13, the intermediate region—which according to the analogy (1.11) would consist of growing ideal spherical blobs—should be more easily observable than in the DC situation.

Our aim here is to show that the results (1.12) and (1.13) are in fact incorrect. Our analysis is based on the following observation.[19] The analogy described by eq 1.11 between cases (a) and (b) is valid only because three-body (as well as higher order) interactions are irrelevant for the isolated chain behavior. In more restricted situations (e.g., a chain confined in a cylindrical pore), three-body interactions may play a role; in such a case, the analogy between a "good solvent of low molecular weight" and a "chemically identical, high molecular weight solvent" breaks down. Indeed, for a good solvent of low molecular weight, the second virial coefficient depends greatly on temperature ($v \cong a^3$ at high temperature, $v \cong a^3(T - \theta)/T$ near the Θ temperature), whereas the third virial coefficient is essentially independent of temperature and of order a^6 (for more details see Appendix 3). For a chemically identical, high molecular weight solvent, however, *both* two-body interactions and three-body interactions are screened out: the second virial coefficient is of order a^3/P, and the third virial coefficient is of order a^6/P (and not a^6!). Therefore, the equivalence (1.10) is an equivalence only between second virial coefficients and as such is only valid in situations where three-body interactions are negligible. In more restricted geometries (like the star case considered in this paper, where each chain is confined in a conical region) three-body interactions may be important and the analogy between a good solvent of low molecular weight and a chemically identical, high molecular weight solvent is invalid.

In order to examine these questions in more detail, it is useful to consider first the case of polymer chains tethered by one end to a flat solid surface. At high enough coverage, the chains stretch away from the surface forming a polymer "brush". In the last 15 years, polymer brushes have been the subject of numerous theoretical and experimental studies.[20] The pioneering work of Alexander and de Gennes,[21,22] based on scaling arguments, was followed more recently by computer simulations[23,24] and self-consistent-field calculations.[25–28] Throughout this paper we adopt the Alexander–de Gennes scaling picture; in particular we assume a steplike concentration profile and impose that all free ends be at the same distance from the surface. While it is now realized that these restrictions should be relaxed,[25–28] Auroy et al. have shown very recently that the scaling picture—which describes each chain as a sequence of blobs—still retains all its interest.[29]

In section 2.1 we consider the case of a polymer brush exposed to a good solvent ($0 < v \leq a^3$) of low molecular weight. The dependence of the brush height on solvent quality was analyzed recently by Halperin[30] and Zhulina et al.[31] These authors were particularly interested in the collapse of the brush caused by a decrease in temperature (i.e., in solvent quality). Here our point of view is slightly different. We keep the temperature constant but increase the grafting density. While many of our results are similar to those obtained in refs 30 and 31, our analysis gives a clear blob picture of the various existing regimes and of the crossovers between them. It also illustrates clearly the respective role played by two-body and three-body interactions.

In section 2.2 we consider the less familiar case of a polymer brush exposed to a melt of chemically identical chains. This case was first considered by de Gennes some years ago.[32-34] In order to emphasize the respective role played by two-body interactions and three-body interactions, we use a virial expansion for the entropy of mixing rather than the full Flory–Huggins expression used by de Gennes. In addition to a Flory-type approach, we also develop a more refined scaling analysis.

Finally, in section 3 we consider the behavior of a star immersed in a solvent of high molecular weight. The paper ends with a short discussion.

2. Polymers Tethered to a Flat Surface

2.1. Good Solvent Case. We first consider the case of polymer chains, with degree of polymerization N, terminally grafted onto a flat surface and exposed to a solvent of low molecular weight. The number of terminally grafted chains per unit area is σa^{-2}, where a is the monomer size. The average distance between two grafting sites is given by $D = a\sigma^{-1/2}$. The solvent quality is characterized by an excluded-volume parameter v satisfying $0 < v \leq a^3$ (good solvent) and a third virial coefficient of order a^6 (see Appendix 3). At low coverage, the different coils do not overlap and each chain occupies roughly a half-sphere with a radius comparable to the Flory radius of a free chain (see eq A1.5)

$$R \cong aN^{3/5}(v/a^3)^{1/5} \tag{2.1}$$

In writing eq 2.1 we have assumed that the chain is long enough to be described as a self-avoiding walk of thermal blobs: $N \gg (v/a^3)^{-2}$. The opposite limit will be considered at the end of section 2.1 (paragraph C).

When the grafting density σ becomes greater than the critical density

$$\sigma_0 \cong (a/R)^2 \cong N^{-6/5}(v/a^3)^{-2/5} \tag{2.2}$$

the different chains begin to overlap and form a brush of height L. The equilibrium structure of the brush results from the competition between osmotic forces that tend to expand the layer and the restoring elastic forces. Accordingly, the free energy per chain can be written as

$$F = F_{os} + F_{el} \tag{2.3}$$

In a Flory-type approach, the elastic free energy is given by

$$\frac{F_{el}}{kT} \cong \frac{L^2}{a^2N} \tag{2.4}$$

while the osmotic free energy is given by

$$\frac{F_{os}}{kT} \cong v\frac{N^2}{LD^2} + a^6\frac{N^3}{(LD^2)^2} \tag{2.5}$$

The first term in eq 2.5 corresponds to the effect of the two-body interactions, while the second term corresponds to three-body interactions.

For a given grafting density, the crossover between these two contributions occurs for $L_{c.o.} \cong aN\sigma(v/a^3)^{-1}$, and the corresponding value of F_{os} is given by $(F_{os}/kT)_{c.o.} \cong N(v/a^3)^2$. Since the equilibrium value of L is obtained by balancing F_{os} with F_{el}, two different regimes must be considered according to the relative value of σ with respect to the critical density σ_1 defined by

$$\frac{L_{c.o.}^{\ 2}}{a^2N} \cong \left(\frac{F_{os}}{kT}\right)_{c.o.} \tag{2.6}$$

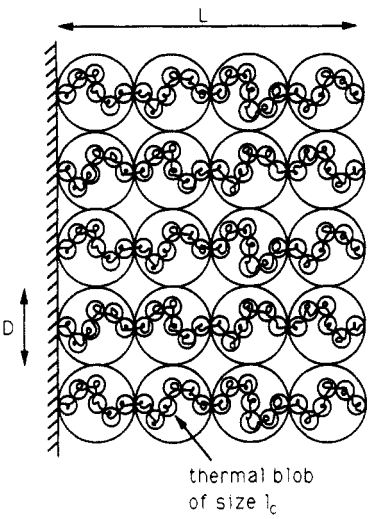

Figure 2. Schematic representation of a polymer brush exposed to a good solvent of low molecular weight in the moderate-coverage regime $\sigma_0 < \sigma < \sigma_1$. In this regime the blob size $D = a\sigma^{-1/2}$ is greater than thermal blob size $l_c \cong a(v/a^3)^{-1}$.

That is

$$\sigma_1 \cong (v/a^3)^2 \tag{2.7}$$

A. Moderate-Coverage Regime. This regime is described by the double inequality

$$\sigma_0 < \sigma < \sigma_1 \tag{2.8}$$

In this regime the contribution of the three-body interactions is negligible and

$$\frac{F}{kT} \cong \frac{L^2}{a^2N} + v\frac{N^2}{LD^2} \tag{2.9}$$

By minimizing eq 2.9, we obtain

$$L \cong aN\sigma^{1/3}(v/a^3)^{1/3} \tag{2.10}$$

and

$$F/kT \cong N\sigma^{2/3}(v/a^3)^{2/3} \tag{2.11}$$

In this moderate-coverage regime, it is possible to develop a more refined scaling analysis, very similar to Alexander's analysis of the athermal solvent case ($v = a^3$).[21] Consider a brush in equilibrium. The fundamental distance of the problem is D, the average distance between two grafting sites. A grafted chain is subdivided into blobs of size D, each containing g_D monomers. Within one blob, the chain behaves like a free excluded-volume chain; this leads to the relation (see eq A1.5)

$$D \cong ag_D^{3/5}(v/a^3)^{1/5} \tag{2.12}$$

Different blobs repel each other, and the brush is essentially a closely packed system of blobs. The monomer volume fraction, ϕ, is given by

$$\phi \cong g_D(a/D)^3 \cong \sigma^{2/3}(v/a^3)^{-1/3} \tag{2.13}$$

Since the volume per grafted chain is LD^2, the monomer volume fraction can be written as

$$\phi \cong Na^3/(LD^2) \cong Na\sigma/L \tag{2.14}$$

Comparing eqs 2.13 and 2.14, we obtain for the equilibrium brush height

$$L \cong aN\sigma^{1/3}(v/a^3)^{1/3} \cong (N/g_D)D \tag{2.15}$$

This last result indicates that the chain can be viewed as a string of blobs almost fully stretched along the normal to the wall (Figure 2). (There is, however, a random-walk

component parallel to the wall plane;[32] for reasons of simplicity, this effect is not represented in Figure 2.)

The kT per blob ansatz leads to a free energy per chain (see also Appendix 4)

$$\frac{F}{kT} \cong \frac{N}{g_D} \cong N\sigma^{5/6}(v/a^3)^{1/3} \tag{2.16}$$

While the Flory analysis gives a correct estimate of the brush height, it overestimates the brush free energy (compare eqs 2.11 and 2.16, keeping in mind the inequality (2.8)).

When the grafting density increases, the blob size D progressively decreases up to a point where it is on the order of the thermal blob size $l_c \cong a(v/a^3)^{-1}$. The crossover occurs for $D \cong a(v/a^3)^{-1}$, that is, for a grafting density $\sigma \cong (v/a^3)^2$. This density is identical to the density σ_1 (eq 2.7) which defines the crossover between the regime dominated by two-body interactions and the regime dominated by three-body interactions. We therefore conclude that, as long as the density is smaller than σ_1 (eq 2.7), the osmotic forces that tend to expand the layer are dominated by two-body interactions and the blob size D is greater than thermal blob size l_c. We now consider what happens at larger grafting densities.

B. High-Coverage Regime. This regime is described by

$$\sigma_1 < \sigma < 1 \tag{2.17}$$

In this regime, we can neglect two-body interactions compared with three-body interactions and the Flory free energy per chain is

$$\frac{F}{kT} \cong \frac{L^2}{a^2N} + a^6\frac{N^3}{(LD^2)^2} \tag{2.18}$$

By minimizing eq 2.18, we obtain

$$L \cong aN\sigma^{1/2} \tag{2.19}$$

and

$$F/kT \cong N\sigma \tag{2.20}$$

The monomer volume fraction can be written as

$$\phi \cong Na\sigma/L \cong \sigma^{1/2} \tag{2.21}$$

This last result shows that the brush is never dry (except for the limiting case $\sigma = 1$), where "dry" means $\phi \cong 1$.

We now construct a blob picture for this high-coverage regime. As for the moderate-coverage regime, the fundamental distance of the problem is given by D, and a grafted chain is subdivided into blobs of size D, each containing g_D monomers. But now, within one blob, the chain behaves like an ideal chain; this leads to the relation

$$D \cong ag_D^{1/2} \tag{2.22}$$

Different blobs repel each other, and the brush is essentially a closely packed system of blobs. The monomer volume fraction, ϕ, is given by

$$\phi \cong g_D(a/D)^3 \cong \sigma^{1/2} \tag{2.23}$$

Comparing eqs 2.23 and 2.14, we obtain for the equilibrium brush height

$$L \cong aN\sigma^{1/2} \cong (N/g_D)D \tag{2.24}$$

This last result indicates that the chain can be viewed as a string of ideal blobs almost fully stretched along the normal to the wall.

The kT per blob ansatz leads to a free energy per chain (see also Appendix 4):

$$F/kT \cong N/g_D \cong N\sigma \tag{2.25}$$

Thus, in the high-coverage regime, the Flory analysis gives a correct estimate of both the brush height and the brush free energy (compare eqs 2.19 and 2.24 and eqs 2.20 and 2.25).

C. Remarks. (1) Up to now we have assumed that the grafted chains were long enough to be described in their free (i.e., ungrafted) state as self-avoiding walks of thermal blobs: $N \gg (v/a^3)^{-2}$. We now consider the opposite limit $N \ll (v/a^3)^{-2}$. Then, at low enough coverage such that the different coils do not overlap, each chain occupies a half-sphere with an ideal radius $R_0 \cong aN^{1/2}$. Let us progressively increase the grafting density σ. When σ becomes greater than the overlap density $\sigma_{over} \cong (a/R_0)^2 \cong N^{-1}$, the different chains begin to overlap and form a brush. Since by assumption $N \ll (v/a^3)^{-2}$, the density σ_{over} is greater than the density σ_1 defined by eq 2.6. We therefore conclude that whenever $\sigma > \sigma_{over} \cong N^{-1}$, the three-body interactions are dominant and the chains can be viewed as linear strings of ideal blobs. The brush height and the free energy per chain are then respectively given by

$$L \cong aN\sigma^{1/2}, \quad F/kT \cong N\sigma \tag{2.26}$$

Note that, for $\sigma \cong \sigma_{over}$, eq 2.26 gives $L \cong R_0$ and $F/kT \cong 1$, as expected.

(2) The brush picture adopted in this paper (steplike concentration profile and all free ends at the same distance from the surface) imposes strong restrictions on the allowed chains configurations. Some years ago, Hirz numerically solved the self-consistent-field (SCF) equations describing the brush situation[25] but relaxing the above-mentioned restrictions. She found that in the case of a good solvent the concentration profile was essentially parabolic. This was rationalized analytically by Milner et al.[26,27] and Zhulina et al.[28] Much of the physics of the parabolic profile may be understood in terms of the following simple argument.[35] The mean-field free energy per unit area of the brush, γ, may be written as

$$\gamma/kT = \int \left[\frac{1}{2}vc^2(x) + \frac{1}{2Na^2}x^2\Psi(x) - \mu c(x)\right] dx \tag{2.27}$$

where $c(x)$ and $\Psi(x)$ are respectively the monomer concentration and the free end concentration at a distance x from the surface. The first two terms in the integral respectively represent the excluded-volume energy and the polymer stretching energy; μ is a Lagrange multiplier to fix N monomers per chain. The problem is to determine $\Psi(x)$. A crude approximation may be obtained by guessing that $\Psi(x) \cong c(x)/N$. Now setting $\delta\gamma/\delta c(x) = 0$, we obtain

$$c(x) = v^{-1}\left[\mu - \frac{1}{2}(x/Na)^2\right] \tag{2.28}$$

where $\mu = [(3/2\sqrt{2})(v/D^2a)]^{2/3}$ and the brush height is consistent with eq 2.15, $L = Na(3v/D^2a)^{1/3}$. The overall parabolic form is clearly evident from eq 2.28. Note that in writing eq 2.27 we have assumed that the osmotic forces were dominated by two-body interactions. From the analysis of section 2.1 we know that this assumption is correct only in the moderate-coverage regime $N^{-6/5}(v/a^3)^{-2/5} < \sigma < (v/a^3)^2$.

In the high-coverage regime ($(v/a^3)^2 < \sigma < 1$), three-body interactions are dominant and the mean-field free

energy (eq 2.27) should be replaced by

$$\gamma/kT = \int \left[\frac{1}{6}a^6c^3(x) + \frac{1}{2Na^2}x^2\Psi(x) - \mu c(x)\right] dx \quad (2.29)$$

Guessing once again that $\Psi(x) \simeq c(x)/N$ and setting $\delta\gamma/\delta c(x) = 0$, we obtain

$$c(x) = \frac{\sqrt{2}}{a^3}\left[\mu - \frac{1}{2}(x/Na)^2\right]^{1/2} \quad (2.30)$$

where $\mu = 2\pi^{-1}(a/D)^2$ and the brush height is consistent with eq 2.19, $L = 2\pi^{-1/2}Na(a/D)$. In the high-coverage regime ($(v/a^3)^2 < \sigma < 1$), the profile is thus elliptical.[27,36]

One final comment on SCF calculations. As we saw in section 2.1.A, the mean-field picture (which ignores the effect of chain correlations) is not very accurate in the moderate-coverage regime $N^{-6/5}(v/a^3)^{-2/5} < \sigma < (v/a^3)^2$ where scaling arguments should be used. Consequently, in this regime, we do not expect the behavior of the grafted chains to be described by the analytic parabolic brush of the "mean-field" SCF theory (this mean-field SCF theory is presented in detail by Milner et al.,[27] section 1) but rather by the "augmented" SCF theory of the same authors[27] (section 3). (The profile predicted by the augmented SCF theory is, however, quite similar to that of the mean-field SCF theory.) Since in the high-coverage regime ($(v/a^3)^2 < \sigma < 1$) we expect the profile to be essentially elliptical, we never expect the analytic parabolic brush of the mean-field SCF theory to describe exactly the brush behavior. This result is in contradiction with the criterion proposed by Milner et al.[26,27] Indeed, according to these authors, when $(v/a^3)^{(d-1)/(4-d)} < \sigma < 1$, with d the dimension of space, one expects the analytic parabolic brush of the mean-field SCF theory to be valid. This discrepancy is probably due to the fact that Milner et al.[26,27] have not considered ternary interactions.

(3) The free energy of a brush under compression is discussed in Appendix 4.

2.2. Melt Case. We now consider the case where the grafted chains (degree of polymerization N) are in contact with a melt of shorter, chemically identical chains (degree of polymerization P, with $P < N$).[32] At low coverage, the different coils do not overlap and each chain occupies roughly a half-sphere with a radius comparable to the Flory radius of a free chain (see eq A2.5)

$$R \simeq aN^{3/5}P^{-1/5} \quad (2.31)$$

In writing eq 2.31 we have assumed that the chains are long enough to be described as self-avoiding walks of *melt blobs*: $N \gg P^2$ (see Appendix 2). The opposite limit ($N \ll P^2$) has been analyzed in detail by de Gennes[32] and will be briefly considered at the end of section 2.2 (paragraph C).

When the grafting density σ becomes greater than the critical density

$$\sigma'_0 \simeq N^{-6/5}P^{2/5} \quad (2.32)$$

the different chains begin to overlap and form a brush of height L. The free energy per chain contains two contributions: (a) an entropy of mixing between the P chains and the N chains, F_{mix}, and (b) an elastic free energy, F_{el}:

$$F = F_{el} + F_{mix} \quad (2.33)$$

In a Flory-type approach, the elastic free energy is given by

$$\frac{F_{el}}{kT} \simeq \frac{L^2}{a^2N} \quad (2.34)$$

while the mixing free energy is given by

$$\frac{F_{mix}}{kT} \simeq \frac{a^3}{P}\frac{N^2}{LD^2} + \frac{a^6}{P}\frac{N^3}{(LD^2)^2} \quad (2.35)$$

The first term in eq 2.35 corresponds to the effect of the two-body interactions while the second term corresponds to three-body interactions (see Appendix 3). For a given grafting density, the crossover between these two contributions occurs for $L_{c.o.} \simeq aN\sigma$ and the corresponding value of F_{os} is given by $(F_{os}/kT)_{c.o.} \simeq NP^{-1}$. Since the equilibrium value of L is obtained by balancing F_{mix} by F_{el}, two different regimes must be considered according to the value of σ.

A. Moderate Coverage Regime. This regime is described by the double inequality

$$\sigma'_0 < \sigma < \sigma'_1 \simeq P^{-1/2} \quad (2.36)$$

In this regime the contribution of the three-body interactions is negligible and

$$\frac{F}{kT} \simeq \frac{L^2}{a^2N} + \frac{a^3}{P}\frac{N^2}{LD^2} \quad (2.37)$$

By minimizing eq 2.37, we obtain

$$L \simeq aNP^{-1/3}\sigma^{1/3} \quad (2.38)$$

and

$$F/kT \simeq NP^{-2/3}\sigma^{2/3} \quad (2.39)$$

From eq 2.38, the N-monomer volume fraction, ϕ_N, is given by

$$\phi_N \simeq Na\sigma/L \simeq P^{1/3}\sigma^{2/3} \quad (2.40)$$

In writing eq 2.35 we have assumed that the volume fraction of the P chains inside the grafted layer is large enough for the interactions between N monomers to be screened. The N-monomer volume fraction should therefore be smaller than 1 ($\phi_N < 1$) for eqs 2.38 and 2.39 to be valid. According to eq 2.40, this implies that the grafting density σ is smaller than $P^{-1/2}$. Note that this density does coincide with the upper bound of the moderate-coverage regime (see eq 2.36). To summarize, in the moderate-coverage regime ($\sigma'_0 < \sigma < \sigma'_1$), some mobile P chains are still present inside the brush (wet brush) and the free energy (eq 2.35) is meaningful; moreover, the second term of this free energy corresponding to three-body interactions plays a negligible role.

We now try to build a blob model for this moderate-coverage regime. Assume that the fundamental distance of the problem is D, the average distance between two grafting sites. A grafted chain may then be subdivided into spherical blobs of size D, each containing g_D monomers. Within one blob, the chain behaves like a free chain; this leads to the relation (see eq A2.5)

$$D \simeq ag_D^{3/5}P^{-1/5} \quad (2.41)$$

Different blobs repel each other, and the brush is essentially a closely packed system of blobs. The N-monomer volume fraction, ϕ_N, is given by

$$\phi_N \simeq g_D(a/D)^3 \simeq \sigma^{2/3}P^{1/3} \quad (2.42)$$

Since on the other hand $\phi_N \simeq Na\sigma/L$, we obtain for the equilibrium brush height

$$L \simeq aNP^{-1/3}\sigma^{1/3} \simeq (N/g_D)D \quad (2.43)$$

This last result indicates that the chain can be viewed as a string of blobs almost fully stretched along the normal to the wall. The kT per blob ansatz leads to a free energy

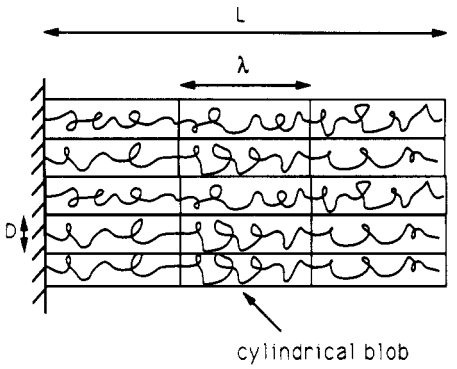

Figure 3. Schematic representation of a polymer brush (N monomers per grafted chain) exposed to a melt of shorter, chemically identical chains (degree of polymerization P, with $P < N$) in the regime $\sigma^* < \sigma < \sigma'_1$. A grafted chain can be viewed as a string of *cylindrical* blobs almost fully stretched along the normal to the wall. Within a blob the chain behaves like an ideal chain (in the direction normal to the wall). The random-walk component parallel to the wall plane is not represented on the figure.

per chain

$$F/kT \cong NP^{-1/3}\sigma^{5/6} \tag{2.44}$$

When the grafting density increases, the blob size D progressively decreases up to a point where it is on the order of the melt blob size $l'_c \cong aP$. The crossover occurs for $D \cong a(v/a^3)^{-1}$; that is, for a grafting density

$$\sigma^* \cong P^{-2} \tag{2.45}$$

It is important to notice that σ^* falls *inside* the moderate-coverage regime

$$\sigma'_0 \cong N^{-6/5}P^{-2/5} < \sigma^* \cong P^{-2} < \sigma'_1 \cong P^{-1/2} \tag{2.46}$$

Consequently, the blob picture (eqs 2.41–2.43) and the resulting scaling free energy (eq 2.44) are only valid for $\sigma'_0 < \sigma < \sigma^*$.

What happens for $\sigma > \sigma^*$? Since D is now smaller than the melt blob size, one might consider describing the chain as a linear string of ideal spherical blobs, each consisting of $g_D \cong (D/a)^2$ monomers. But if we adopt this picture, the brush height is given by

$$L \cong (N/g_D)D \cong aN\sigma^{1/2} \tag{2.47}$$

in disagreement with the Flory result (eq 2.38)!

In order to solve that problem, we conjecture that for $\sigma > \sigma^*$ the brush structure may be described in terms of ideal *cylindrical* blobs (Figure 3).[37] We assume that the blob diameter is given by D. Let Λ be the length of the blob and q the number of monomers per blob. Since within a blob the chain behaves like an ideal chain (in the direction normal to the wall), one has $\Lambda \cong aq^{1/2}$. In order to achieve mutual exclusion between the blobs, the number of monomers per blob should satisfy (see the mixing term in the free energy (eq 2.37))

$$\frac{a^3}{P}\frac{q^2}{\Lambda D^2} \cong 1 \tag{2.48}$$

This leads to

$$q \cong P^{2/3}(D/a)^{4/3} \cong P^{2/3}\sigma^{-2/3} \tag{2.49}$$

$$\Lambda \cong aq^{1/2} \cong aP^{1/3}\sigma^{-1/3} \tag{2.50}$$

Since the different blobs repel each other, the brush height is given by

$$L \cong (N/q)\Lambda \cong aNP^{-1/3}\sigma^{1/3} \tag{2.51}$$

in agreement with the Flory result (eq 2.38).

The kT per blob ansatz leads to a free energy per chain

$$\frac{F}{kT} \cong \frac{N}{q} \cong NP^{-2/3}\sigma^{2/3} \tag{2.52}$$

To summarize, for the moderate-coverage regime $\sigma'_0 < \sigma < \sigma'_1$, the Flory scheme predicts

$$L \cong aNP^{-1/3}\sigma^{1/3} \tag{2.53}$$

and

$$F/kT \cong NP^{-2/3}\sigma^{2/3} \tag{2.54}$$

The scaling analysis gives the same expression for the brush height but a more refined evaluation of the free energy

$$F/kT \cong NP^{-1/3}\sigma^{5/6} \qquad \sigma'_0 < \sigma < \sigma^* \tag{2.55}$$

$$F/kT \cong NP^{-2/3}\sigma^{2/3} \qquad \sigma^* < \sigma < \sigma'_1 \tag{2.56}$$

Note that in the regime $\sigma'_0 < \sigma < \sigma^*$, the Flory scheme overestimates the brush free energy (compare eqs 2.44 and 2.55).

We now consider what happens at larger grafting densities ($\sigma > \sigma'_1$).

B. High-Coverage Regime. This regime is described by

$$\sigma'_1 < \sigma < 1 \tag{2.57}$$

In this regime the P chains are almost completely expelled from the brush and the height L is related to the grafting density σ by the requirement

$$\phi_N \cong Na\sigma/L \cong 1 \tag{2.58}$$

Equation 2.58 leads to

$$L \cong Na\sigma \tag{2.59}$$

The free energy per chain consists merely of an elastic term

$$\frac{F}{kT} \cong \frac{L^2}{a^2N} \cong N\sigma^2 \tag{2.60}$$

One can check that eqs 2.53 and 2.59, as well as eqs 2.56 and 2.60, do coincide for $\sigma \cong \sigma'_1$.

C. Remarks. Up to now we have assumed that the grafted chains were long enough to be described in their free (i.e., ungrafted) state as self-avoiding walks of melt blobs: $N \gg P^2$. We now consider the opposite limit $N \ll P^2$.[32] At low enough coverage for the different coils not to overlap, each chain occupies a half-sphere with an ideal radius $R_0 \cong aN^{1/2}$. Let us progressively increase the grafting density σ. When σ becomes greater than the overlap density $\sigma_{over} \cong (a/R_0)^2 \cong N^{-1}$, the different chains begin to overlap and form a brush of height L. Since by assumption $N \ll P^2$, the overlap density σ_{over} is greater than the density σ^* (eq 2.45). One might therefore conclude that, whenever $\sigma > \sigma_{over}$, the brush height and the free energy per chain are respectively given by eqs 2.53 and 2.56. But if we evaluate the value of eq 2.53 for $\sigma \cong \sigma_{over}$, we obtain $L \cong aN^{2/3}P^{-1/3}$ which is smaller than the expected crossover value $L \cong R_0 \cong aN^{1/2}$! This result simply indicates that for $\sigma \cong \sigma_{over}$ the two-body interactions are not sufficient to swell the chains.[32] Thus, up to a certain threshold density σ_{thre}, the brush height remains equal to R_0. The density σ_{thre} can be obtained as follows. From the mixing term in the free energy (eq 2.37), one can define a perturbation parameter ξ as

$$\xi \cong \frac{a^3}{P}\frac{N^2}{R_0D^2} \cong \sigma N^{3/2}P^{-1} \tag{2.61}$$

The threshold density σ_{thre} is then simply obtained by

setting $\xi \cong 1$; thus

$$\sigma_{thre} \cong N^{-3/2}P \tag{2.62}$$

For $\sigma > \sigma_{thre}$, the brush is stretched and

$$L \cong aNP^{-1/3}\sigma^{1/3} \tag{2.63}$$

$$F/kT \cong NP^{-2/3}\sigma^{2/3} \tag{2.64}$$

Note that, for $\sigma \cong \sigma_{thre}$, eqs 2.63 and 2.64 give $L \cong R_0$ and $F/kT \cong 1$, as expected.

At higher densities, we reach the crossover $\sigma'_1 \cong P^{-1/2}$ above which the brush is almost dry. For $\sigma > \sigma'_1$, the brush height and the free energy per chain are respectively given by eqs 2.59 and 2.60.

3. Star Polymer in High Molecular Weight Solvents

We now investigate the static behavior of star polymers dissolved in high molecular weight solvents. Consider a star polymer made of f identical arms. Each arm consists of N monomers of size a. The star is immersed in a melt of linear chains, chemically identical to the star arms, with degree of polymerization $P < N$. Let us first consider what happens in the outer region of the star, far away from the center. Following the idea of Daoud and Cotton,[1] we describe each arm as a succession of growing spherical blobs. At a given distance r from the center, there are f blobs, one for each polymer chain. Since f blobs cover a sphere of radius r, the blob radius is given by

$$\xi(r) \cong rf^{-1/2} \tag{3.1}$$

Within one blob, the arm behaves as an isolated chain. According to eq A2.5 of Appendix 1, the number $n(r)$ of monomer per blob of size $\xi(r)$ is then given by

$$\xi(r) \cong an(r)^{3/5}P^{-1/5} \tag{3.2}$$

Combining eqs 3.1 and 3.2, we obtain for the N-monomer volume fraction

$$\phi_N(r) \cong n(r)/\xi^3(r) \cong (r/a)^{-4/3}f^{2/3}P^{1/3} \tag{3.3}$$

Equation 3.2 is valid as long as the blob size $\xi(r) \cong rf^{-1/2}$ is larger than the size of a *melt* blob $l'_c \cong aP$ introduced in the Appendix 2. Consequently, eqs 3.1 and 3.2 are valid only in the outer part of the star. This region is defined by $r \geq r'_1$ with

$$r'_1 \cong af^{1/2}P \tag{3.4}$$

For distances smaller than r'_1, we picture each arm as a succession of growing *ideal cylindrical* blobs (see Figure 4), following the ideas introduced in section 2.2.A. At a given distance r from the center, there are f cylindrical blobs, one for each polymer chain. Since the f blobs cover a sphere of radius r, the blob diameter, $D(r)$, is given by

$$D(r) \cong rf^{-1/2} \tag{3.5}$$

Let $\Lambda(r)$ be the length of the blob and $q(r)$ the number of monomers inside the blob. Since within the blob the chain behaves ideally (in the direction parallel to the blob axis), the length of the blob is related to $q(r)$ by

$$\Lambda(r) \cong aq^{1/2}(r) \tag{3.6}$$

The number of monomers per blob is such to achieve mutual exclusion between the different blobs. According to eq 2.49, we thus have

$$q(r) \cong P^{2/3}(D(r)/a)^{4/3} \cong (r/a)^{4/3}f^{-2/3}P^{2/3} \tag{3.7}$$

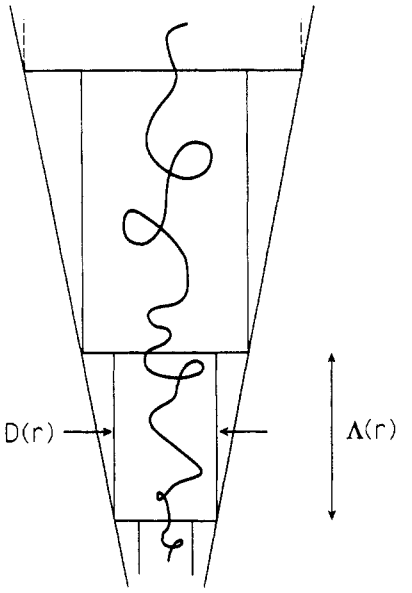

Figure 4. Schematic representation of the region $r'_1 < r < r'_2$ for a star polymer (N monomers per arm) dissolved in a melt of shorter, chemically identical chains (degree of polymerization P, with $P < N$). Each arm can be pictured as a succession of growing cylindrical blobs. Within a blob the chain behaves like an ideal chain (in the radial direction).

Consequently (see eq 3.6)

$$\Lambda(r) \cong a(r/a)^{2/3}f^{-1/3}P^{1/3} \tag{3.8}$$

Combining eqs 3.5, 3.7, and 3.8, we obtain for the N-monomer volume fraction

$$\phi_N(r) \cong a^3q(r)/(\Lambda(r)\,D(r)^2) \cong (r/a)^{-4/3}f^{2/3}P^{1/3} \tag{3.9}$$

Note that this expression is identical to the volume fraction in the swollen regime $r > r'_1$ (eq 3.3)! We therefore conclude that, while the nature of the blobs changes for $r \cong r'_1$, the volume fraction $\phi_N(r)$ keeps the same form above and below r'_1.

For smaller values of r, we reach a distance r'_2 below which the N-monomer volume fraction is unity ($\phi_N \cong 1$). From eq 3.9 we get

$$r'_2 \cong af^{1/2}P^{1/4} \tag{3.10}$$

Therefore, according to our model, the N-monomer volume fraction is given by

$$\phi_N(r) \cong 1 \qquad r < af^{1/2}P^{1/4} \tag{3.11a}$$

$$\phi_N(r) \cong (r/a)^{-4/3}f^{2/3}P^{1/3} \qquad af^{1/2}P^{1/4} < r < R \tag{3.11b}$$

The radius of the star, R, can be deduced from the condition

$$Nfa^3 = \int_0^R \mathrm{d}^3r\,\phi_N(r) \tag{3.12}$$

Using eqs 3.11 and 3.12, one obtains

$$R \cong aN^{3/5}f^{1/5}P^{-1/5} \qquad N \gg f^{1/2}P^{3/4} \tag{3.13a}$$

$$R \cong aN^{1/3}f^{1/3} \qquad N \ll f^{1/2}P^{3/4} \tag{3.13b}$$

The results (3.13a) and (3.13b) for the star radius can also be obtained from a simple Flory-type free energy, as explained in Appendix 5.

The free energy of a star with $N \gg f^{1/2}P^{3/4}$ can be written as the sum of two contributions due to the inner meltlike region (the "core", $r < r'_2$) and the remaining of the star

(the "corona", $r'_2 < r < R$)

$$F_{star} = F_{core} + F_{corona} \tag{3.14}$$

The free energy of the corona is given by the kT per blob ansatz

$$F_{corona}/kT \cong \int_{r'_2}^{r'_1} \frac{d^3r}{\Lambda(r)\, D^2(r)} + \int_{r'_1}^{R} \frac{d^3r}{\xi^3(r)} \tag{3.15}$$

Using eqs 3.1–3.10, we obtain

$$F_{corona}/kT \cong f^{3/2} \ln(N^{3/5}P^{-6/5}f^{-3/10}) \qquad f^{1/2}P^2 \ll N \tag{3.16a}$$

$$F_{corona}/kT \cong N^{1/5}P^{-2/5}f^{7/5} \qquad f^{1/2}P^{3/4} \ll N \ll f^{1/2}P^2 \tag{3.16b}$$

Note that eqs 3.16a and 3.16b do coincide for $N \cong f^{1/2}P^2$ if one approximates the logarithmic factors in eq 3.16a as a constant.

F_{core} accounts for the stretching penalty in the inner meltlike region. A very crude evaluation of F_{core} may be obtained by assuming that for each arm the part of the chain inside the core ($f^{1/2}P^{3/4}$ monomers) is stretched to an end-to-end distance on the order of the core radius

$$F_{core}/kT \cong f\left(\frac{a(f^{1/2}P^{3/4})^{1/3}f^{1/3}}{af^{1/4}P^{3/8}}\right)^2 \cong f^{3/2}P^{-1/4} \tag{3.17}$$

We now briefly consider the force, $F(h)$, between two stars separated by a distance h.[38] We assume $N \gg f^{1/2}P^{3/4}$. In the limit $r'_2 \ll h \ll R$ (where r'_2 and R are respectively given by eqs 3.10 and 3.13a), the interstar force may be obtained by integrating the normal component of the osmotic pressure over the symmetry plane (assuming no change in the structure of the stars).[39] Using the fact that the osmotic pressure, $\Pi(r)$, is given by

$$\Pi(r) \cong kT/\xi^3(r) \qquad r'_1 \ll r \ll R \tag{3.18a}$$

$$\Pi(r) \cong kT/\Lambda(r)D^2(r) \qquad r'_2 \ll r \ll r'_1 \tag{3.18b}$$

where $\xi(r)$, $D(r)$, and $\Lambda(r)$ are respectively given by eqs 3.1, 3.5, and 3.8, we obtain

$$F(h) \cong \frac{kT}{a} f^{3/2}\left(\frac{a}{h}\right) \qquad r'_1 \ll h \ll R \tag{3.19a}$$

$$F(h) \cong \frac{kT}{a} f^{4/3}P^{-1/3}\left(\frac{a}{h}\right)^{2/3} \qquad r'_2 \ll h \ll r'_1 \tag{3.19b}$$

One can easily check that eqs 3.19a and 3.19b do coincide for $r \cong r'_1$. If $f^{1/2}P^{3/4} \ll N \ll f^{1/2}P^2$, the radius R is smaller than r'_1 and only the regime (3.19b) is seen.

It is of importance to note that the expression (3.18b) corresponds to the mean-field form for the osmotic pressure.[39] Indeed, using eqs 3.5 and 3.8, we obtain

$$\Pi(r) \cong kT/\Lambda(r)\, D^2(r) \cong P^{-1}[\phi_N(r)]^2 \tag{3.20}$$

where $\phi_N(r)$ is the N-monomer volume fraction eq 3.11b. Equation 3.20 is identical to the mean-field form for the osmotic pressure predicted by the Flory–Huggins free energy (eq A3.3).

4. Concluding Remarks

(1) In the last section (section 3) we have considered the static properties of a single star polymer dissolved in a high molecular weight solvent. We now briefly consider concentration effects, following closely the analysis of Daoud and Cotton.[1] The overlap concentration above which the different stars begin to overlap is given by $c^* \cong Nf/R^3$. Assuming that $N \gg f^{1/2}P^{3/4}$, we obtain from eq 3.13a

$$c^* \cong a^{-3}N^{-4/5}f^{2/5}P^{3/5} \tag{4.1}$$

For $c > c^*$, arms of different stars entangle and the solution can be pictured as follows: around the center of a given star there is a region of size $\chi(c)$ where the star has a single star behavior. $\chi(c)$ is defined by the equality $\phi_N(r=\chi(c)) \cong ca^3$ where $\phi_N(r)$ is the single star monomer volume fraction (see section 3). According to eq 3.11b, we obtain

$$\chi(c) \cong a(ca^3)^{-3/4}P^{1/4}f^{1/2} \tag{4.2}$$

Note that the use of eq 3.11b is valid as long as $\chi(c)$ (eq 4.2) is larger than r'_2, i.e., up to concentrations of order unity. For $r > \chi(c)$, the solution locally looks like a semidilute solution of linear polymers (in a high molecular weight solvent) with a concentration c and can be characterized by a correlation length[40]

$$\xi(c) \cong a(ca^3)^{-3/4}P^{1/4} \tag{4.3}$$

The total star radius is by

$$R_{star} \cong \chi(c) + \Lambda \tag{4.4}$$

with

$$\Lambda^2 \sim (N-n)a^2(ca^3)^{-1/4}P^{-1/4} \tag{4.5}$$

Here n is the number of monomers (per arm) within the region of size χ:

$$\chi(c) \cong an^{3/5}f^{1/5}P^{-1/5} \tag{4.6}$$

For $c^* < c < f^{2/5}c^*$, $R_{star} \sim \chi$, while for much higher concentrations ($c \gg f^{2/5}c^*$) we expect $R_{star} \sim aN^{1/2}\cdot(ca^3)^{-1/8}P^{-1/8}$.

The DC analysis for a solution of f-armed star polymers in a good solvent of low molecular weight[1] has been extended by Witten et al.[38,41] to allow a calculation of the scaling regimes of the osmotic pressure, Π. These authors found a sharp increase in Π at the concentration where the stars begin to overlap. This jump in the osmotic pressure engenders a peak in the scattering structure factor $S(q)$, whose height scales as $f^{3/2}$. Similar effects are expected here. We follow closely the analysis of refs 38 and 41. In the dilute regime $c \ll c^*$ (with c^* given by eq 4.1), the osmotic pressure is of order kT per star:

$$\Pi = kT(c/fN) \tag{4.7}$$

Above c^*, the arms entangle and locally resemble a semidilute linear polymer solution (in a high molecular weight solvent) where the osmotic pressure is given by

$$\Pi = kT/\xi^3 \tag{4.8}$$

$\xi(c)$ is given by eq 4.3. For $c = c^*$, eq 4.8 gives $\Pi = f^{3/2}c^*/(Nf)$. This is a factor $f^{3/2}$ larger than the osmotic pressure calculated from eq 4.7. This implies a relatively rapid change in $\Pi(c)$ in the neighborhood of c^*: in order to pass from the dilute regime to the semidilute one, one must supply sufficient pressure to overcome the osmotic pressure within each star. One can show[38,41] that this steep rise in the osmotic pressure leads to a peak in the scattering structure factor in the vicinity of $q \cong R^{-1}$ (R is the star radius (eq 3.13a)) of relative amplitude $S(q=R^{-1})/S(0) \cong f^{3/2}$ (independent of both N and P). A corollary of the strong peak in the structure factor is the possibility of a crystalline order in the star solution at c^*. Since the peak relative amplitude depends only on the star functionality, f, one expects a crystalline ordering of the polymers when f exceeds a threshold f_c. If following ref 38 we apply the empirical Verlet criterion that simple fluids order when

the peak in the structure factor reaches approximately 3–4, we expect crystallinity with only a few arms (a glassy phase might of course intervene).

(2) Throughout this paper we have emphasized the role of three-body interactions for tethered chains and the resulting lack of analogy between a good solvent of low molecular weight and a chemically identical, high molecular weight solvent. In the tethered situations studied in this paper, three-body interactions become important at high grafting densities for a good solvent of low molecular weight, whereas they remain negligible for a chemically identical, high molecular weight solvent. This explains for example why a flat grafted layer (chains tethered by one end to a surface) in contact with a good solvent ($0 < v \leq a^3$) of low molecular weight is never dry (section 2.1), whereas a flat grafted layer in contact with a melt of shorter, chemically identical chains expels the mobile chains above a critical grafting density (section 2.2). Another consequence concerns the behavior of star polymers (chains tethered by one end to a point). For a star polymer dissolved in a good solvent of low molecular weight ($0 < v \leq a^3$), the Daoud–Cotton model[1] predicts the existence of three regions inside the star: (1) an inner meltlike region, (2) an intermediate region where each arm can be pictured as a succession of growing ideal, spherical blobs, and (3) an outer region where the growing, spherical blobs are swollen. It is clear from the study of section 2.1.C that the mutual exclusion between the different ideal, spherical blobs in the intermediate regime is due to three-body interactions. In the case of a star dissolved in a melt, however (section 3), three-body interactions play no role and one has to group a sufficient number of monomers into cylindrical blobs in order to get a "two-body" energy per blob of order kT.

Acknowledgment. The concept of *cylindrical* blob introduced in section 2.2 emerged from the work of Françoise Brochard-Wyart and one of us on molten polymers in small pores.[37] We thank her and Richard Ross for very useful discussions. E.R. and G.H.F. are grateful to the NSF for support under Grants DMR 01-00033 (E.R.) and DMR 90-57147 (G.H.F.). P.P. is grateful to the DOE for support under Grant FG03-87ER45288. We thank the reviewers for their very interesting comments.

Appendix 1. Behavior of an Isolated Linear Chain in a Good Solvent of Low Molecular Weight

Consider an isolated linear chain, with degree of polymerization N, dissolved in a solvent of low molecular weight.[42] The effective interaction between two monomers may be described by an excluded-volume parameter v. At high temperature v is expected to be proportional to the monomer volume a^3, while v is negative a low temperature. The temperature at which $v = 0$ is called the Θ temperature.

Throughout the paper we adopt the following terminology to describe the solvent quality:

$0 < v \leq a^3$ good solvent

$v = 0$ Θ solvent

$v < 0$ poor solvent

Note that we use the expression good solvent in a rather broad sense: it describes not only the limiting case of a very good or athermal solvent ($v = a^3$) but also the whole range of moderately good solvents ($0 < v < a^3$).

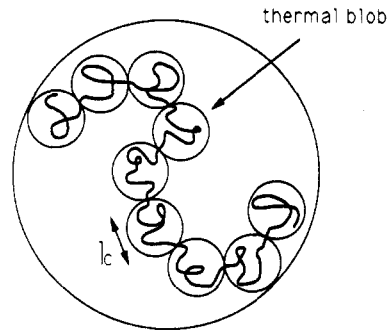

Figure 5. Conformation of one single, partially swollen chain of N monomers dissolved in a good solvent of low molecular weight ($0 < v < a^3$). The chain can be described as a self-avoiding walk of N/N_c thermal blobs of size $l_c = aN_c^{1/2} \cong a(v/a^3)^{-1}$.

In a Θ solvent the chain is ideal with a radius given by the random-walk result

$$R_0 \cong aN^{1/2} \tag{A1.1}$$

Following Flory, the free energy of the chain in a good solvent can be written as

$$F/kT \cong Nv\bar{C} + (R/R_0)^2 \tag{A1.2}$$

where $v\bar{C}$ is the repulsive energy per monomer, $\bar{C}$ being the mean concentration $\bar{C} \cong N/R^3$. The second term in eq A1.2 is an elastic term corresponding to a chain elongation R. From eq A1.2 one can define a perturbation parameter ζ which tells us whether the chain is ideal or not:

$$\zeta \cong Nv\bar{C}_0 \cong vN^2/R_0^3 \cong vN^{1/2} \tag{A1.3}$$

where $\bar{C}_0 \cong N/R_0^3$ is the mean concentration for an ideal chain. If $N < N_c$, with

$$N_c \equiv (v/a^3)^{-2} \tag{A1.4}$$

the perturbation parameter ζ is small and the chain is ideal ($R \cong R_0$). On the other hand, if $N > N_c$, the chain is partially swollen (Figure 5): the short segment of the chain (with a number of monomers smaller than N_c) will show internal correlation of an ideal chain, but larger segments repel each other. The chain thus behaves like a string of subunits, usually called *thermal blobs*, each containing N_c monomers. Within one thermal blob the behavior is ideal, leading to a blob size

$$l_c \cong aN_c^{1/2} \cong a(v/a^3)^{-1} \tag{A1.5}$$

Different thermal blobs repel each other, and the resulting self-avoiding chain (of unit step l_c) has a size

$$R \cong (N/N_c)^{\nu} l_c \cong aN^{3/5}(v/a^3)^{1/5} \tag{A1.6}$$

where $\nu = {}^3/_5$ is the Flory three-dimensional exponent. The result (A1.6) can also be directly obtained by minimizing eq A1.2.

Note that in the limiting case of an athermal solvent ($v = a^3$) the thermal blob consists of a single monomer ($N_c \cong 1$) and the chain is swollen at any length scale.

Appendix 2. Behavior of an Isolated Linear Chain Dissolved in a Melt of Shorter, Chemically Identical Chains

Consider an isolated linear chain, with degree of polymerization N, dissolved in a melt of shorter, chemically identical chains with degree of polymerization P. The bare monomer–monomer interactions of the N chain—described by an excluded-volume parameter a^3—are screened out by the P chains, and the effective excluded-

volume parameter is given by a^3/P. This result was first stated by Flory,[42] but its physical interpretation in terms of screening is due to Edwards.[43] It can be simply deduced from the Flory–Huggins free energy of polymer mixtures.[44] For two chemically identical polymers, the free energy of mixing (per site) is purely entropic:

$$\frac{F_{site}}{kT} = \frac{\phi_N}{N} \ln \phi_N + \frac{1-\phi_N}{P} \ln(1-\phi_N) \qquad (A2.1)$$

where ϕ_N is the volume fraction of the N monomers. In the limit of small ϕ_N, eq A2.2 leads to

$$\frac{F_{site}}{kT} = \frac{\phi_N}{N} \ln \phi_N + \frac{1}{2P}\phi_N^2 + ... \qquad (A2.2)$$

Equation A2.2 shows that the excluded-volume parameter is indeed given by a^3/P.

The Flory free energy of the chain can be written as

$$F/kT \cong \frac{a^3}{P}\frac{N^2}{R^3} + \left(\frac{R}{aN^{1/2}}\right)^2 \qquad (A2.3)$$

The first term of eq A2.3 is a repulsive term due to the screened excluded-volume interaction. The second is an elastic deformation energy. From eq A1.3 we deduced that, if $N < N'_c$, with

$$N'_c \equiv P^2 \qquad (A2.4)$$

the N chain is ideal ($R \cong aN^{1/2}$). On the other hand, if $N > N'_c$, the N chain is partially swollen and behaves like a string of subunits, each of N'_c monomers. Throughout this paper, we will refer to these subunits as *melt blobs*. Within one melt blob the behavior is ideal, and the subunit size is $l'_c = aN'^{1/2}_c = aP$. Different melt blobs repel each other, and the resulting self-avoiding walk of unit step $aN'^{1/2}_c$ has a size

$$R \cong (N/N'_c)^{3/5} l'_c \cong aN^{3/5}P^{-1/5} \qquad (A2.5)$$

Note that, in the limiting case $P = 1$, the melt blob consists of a single monomer ($N'_c \cong 1$) and the chain is swollen at any length scale.

If we compare the results of Appendices 1 and 2, we note that there exists an analogy between (a) the behavior of an isolated linear chain (N monomers) in a good solvent of low molecular weight ($0 < v \leq a^3$) and (b) the behavior of an isolated chain (N monomers) dissolved in a melt of shorter (P monomers, with $P < N$), chemically identical chains.[45] One moves from one case to another simply by using the substitution:

$$(v/a^3)^{-1} \leftrightarrow P \qquad (A2.6)$$

Appendix 3. Third Virial Coefficient

In the preceding two appendices, we have been mainly concerned with two-body interactions. In this appendix, we calculate the value of the third virial coefficient within the framework of the Flory–Huggins theory, both for a linear chain dissolved in a low molecular weight solvent and for a linear chain dissolved in a melt.

A. Linear Chain in a Solvent of Low Molecular Weight. Consider an isolated linear chain, with degree of polymerization N, dissolved in a solvent of low molecular weight. In order to evaluate the value of the third virial coefficient, we use the Flory–Huggins free energy of mixing (per site)

$$\frac{F_{site}}{kT} = \frac{\phi}{N} \ln \phi + (1-\phi) \ln(1-\phi) + \chi\phi(1-\phi) \qquad (A3.1)$$

where ϕ is the monomer volume fraction and χ the usual Flory interaction parameter. In the limit of small ϕ, eq A3.1 leads to

$$\frac{F_{site}}{kT} = \frac{\phi}{N} \ln \phi + \frac{1}{2}(1-2\chi)\phi^2 + \frac{1}{6}\phi^3 + ... \qquad (A3.2)$$

From eq A3.2 we deduce that (i) the excluded-volume parameter defined in Appendix 1 is related to the Flory interaction parameter by $v = a^3(1-2\chi)$ and (ii) the third virial coefficient is given by a^6. Note that while the second virial coefficient v depends on temperature, the third virial coefficient is temperature independent. In particular, for the case of a moderately good solvent ($0 < v < a^3$), the second virial coefficient is smaller than a^3 while the third virial is equal to a^6.

B. Linear Chain in a Melt of Shorter, Chemically Identical Chains. We now consider an isolated linear chain, with degree of polymerization N, dissolved in a melt of shorter, chemically identical chains, with degree of polymerization P. By expending the Flory–Huggins free energy of mixing (eq A2.1) to third order in the N-monomer volume fraction, ϕ_N, we obtain

$$\frac{F_{site}}{kT} = \frac{\phi_N}{N} \ln \phi_N + \frac{1}{2P}\phi_N^2 + \frac{1}{6P}\phi_N^3 + ... \qquad (A3.3)$$

In addition to the fact that the second virial coefficient (i.e., the excluded-volume parameter) is given by a^3/P, eq A3.3 also indicates that the third virial coefficient is equal to a^6/P. In other words, the bare monomer–monomer–monomer interactions of the N chain, described by a coefficient a^6, are also screened out by the P chains and the effective third virial coefficient is given by a^6/P. More generally, if we go back to eq A2.1, it is easily seen that, for an isolated linear chain dissolved in a melt of shorter, chemically identical chains, all the virial coefficients are screened out.

Appendix 4. Brushes under Compression

The equilibrium properties of a polymer brush exposed to a good solvent ($0 < v \leq a^3$) of low molecular weight were analyzed in section 2.1. For the sake of completeness, we here briefly consider the scaling free energy of a brush under compression. Assume that the brush is compressed to a thickness L' smaller than its equilibrium value L (as it would be in a surface force apparatus). According to the value of the grafting density, σ, two regimes must be considered.

(a) Moderate-Coverage Regime. $N^{-6/5}(v/a^3)^{-2/5} < \sigma < (v/a^3)^2$. In this regime the osmotic forces are dominated by two-body interactions (see section 2.1 A) and the brush free energy (per chain) is given by

$$\frac{F}{kT} \cong (v/a^3)^{3/4}(a/L')^{5/4}N^{9/4}\sigma^{5/4} + (v/a^3)^{-1/4}(L'/a)^{7/4}N^{-3/4}\sigma^{-3/4} \qquad (A4.1)$$

The two terms respectively represent the osmotic free energy and the elastic free energy.

One can easily check that minimizing eq A4.1 with respect to L' gives us the equilibrium brush height (2.15) and the corresponding free energy (2.16).

(b) High-Coverage Regime. $(v/a^3)^2 < \sigma < 1$. In this regime the osmotic forces are dominated by three-body interactions (see section 2.1.B) and the brush free energy (per chain) is given by

$$\frac{F}{kT} \cong (a/L')^2N^3\sigma^2 + (L'/a)^2N^{-1} \qquad (A4.2)$$

One can easily check that minimizing eq A4.2 with respect to L' gives us the equilibrium brush height (2.24) and the corresponding free energy (2.25).

Appendix 5. Flory-Type Theory for Star Polymers

In this appendix we use a Flory-type free energy to derive the radius of a star polymer (eqs 1.10a–c and eq 3.13a,b). A similar approach has already been used by Daoud and Cotton.[1]

A. Let us first consider the case of star polymer immersed in a good solvent of low molecular weight. In a crude Flory-type approach, the star free energy has two contributions:

elastic contribution

$$\frac{F_{el}}{kT} \cong f\frac{R^2}{a^2N} \tag{A5.1}$$

interaction contribution

$$\frac{F_{int}}{kT} \cong v\frac{(fN)^2}{R^3} + a^6\frac{(fN)^3}{R^6} \tag{A5.2}$$

Minimizing the star free energy $F_{el} + F_{int}$ leads to the following results:

(i) If $N > f^{1/2}(v/a^3)^{-2}$, the interaction contribution (eq A5.2) is dominated by two-body interactions and $R \cong aN^{3/5}f^{1/5}(v/a^3)^{1/5}$.

(ii) If $f^{1/2} < N < f^{1/2}(v/a^3)^{-2}$, the interaction contribution (eq A5.2) is dominated by three-body interactions and $R \cong aN^{1/2}f^{1/4}$.

(iii) If $N < f^{1/2}$, the star is entirely collapsed and $R \cong aN^{1/3}f^{1/3}$.

From the above results we deduce that a star with long arms ($N > f^{1/2}(v/a^3)^{-2}$) consists of three regions delimited by the radii $r_2 \cong af^{1/2}$, $r \cong af^{1/2}(v/a^3)^{-1}$, and $R \cong aN^{3/5}f^{1/5}(v/a^3)^{1/5}$. In the intermediate region ($r_2 \ll r \ll r_1$) three-body interactions dominate over two-body interactions. Note that it is essential to keep the term $a^6(fN)^3/R^6$ in eq A5.2 in order to recover the intermediate region.

B. We now consider the case of a star polymer dissolved in a high molecular weight solvent. The Flory free energy of the star is given by

$$\frac{F}{kT} \cong f\frac{R^2}{a^2N} + \frac{a^3}{P}\frac{(fN)^2}{R^3} + \frac{a^6}{P}\frac{(fN)^3}{R^6} \tag{A5.3}$$

Minimizing the free energy (eq A5.3) leads to the following results:

(i) If $N > f^{1/2}P^{3/4}$, the interaction contribution is dominated by two-body interactions and $R \cong aN^{3/5}f^{1/5}P^{-1/5}$.

(ii) If $N < f^{1/2}P^{3/4}$, the star is entirely collapsed and $R \cong aN^{1/3}f^{1/3}$.

We deduce that a star with long arms ($N > f^{1/2}P^{3/4}$) consists of only two regions delimited by the radii $af^{1/2}P^{1/4}$ and $aN^{3/5}f^{1/5}P^{-1/5}$. The absence of an intermediate region has its origin in the fact that for three-body interactions to be dominant (over two-body interactions) the N-monomer volume fraction should be of order unity, as easily seen from eq A5.3.

References and Notes

(1) Daoud, M.; Cotton, J. P. *J. Phys. (Paris)* **1982**, *43*, 531.
(2) Burchard, W. *Adv. Polym. Sci.* **1983**, *48*, 1.
(3) Miyake, A.; Freed, K. F. *Macromolecules* **1983**, *16*, 1228.
(4) Birshtein, T. M.; Zhulina, E. B. *Polymer* **1984**, *25*, 1453.
(5) Freire, J. J.; Rey, A.; Garcia de la Torre, J. *Macromolecules* **1986**, *19*, 457.
(6) Witten, T. A.; Pincus, P.; Cates, M. E. *Europhys. Lett.* **1986**, *2*, 137.
(7) Lipson, J. E. G.; Gaunt, D. S.; Wilkinson, M. K.; Whittington, S. G. *Macromolecules* **1987**, *20*, 186.
(8) Halperin, A.; Alexander, S. *Macromolecules* **1987**, *20*, 1146.
(9) Grest, G. S.; Kremer, K.; Witten, T. A. *Macromolecules* **1987**, *20*, 1376.
(10) Khasat, N.; Pennisi, R. W.; Hadjichristidis, N.; Fetters, L. J. *Macromolecules* **1988**, *21*, 1100.
(11) Richter, D.; Farago, B.; Huang, J. S.; Fetters, L. J.; Ewen, B. *Macromolecules* **1989**, *22*, 486.
(12) Grest, G. S.; Kremer, K.; Milner, S. T.; Witten, T. A. *Macromolecules* **1989**, *22*, 1904.
(13) Boothroyed, A. T.; Squires, G. L.; Fetters, L. J.; Rennie, A. R.; Horton, J. C.; de Vallêra, A. M. *Macromolecules* **1989**, *22*, 3130.
(14) Batoulis, J.; Kremer, K. *Macromolecules* **1989**, *22*, 4277.
(15) Dozier, W. D.; Huang, J. S.; Fetters, L. J. *Macromolecules* **1991**, *24*, 2810.
(16) Halperin, A.; Joanny, J. F. *J. Phys. II* **1991**, *1*, 623.
(17) Adam, M.; Fetters, L. J.; Graessely, W. W.; Witten, T. A. *Macromolecules* **1991**, *24*, 2434.
(18) Alessandrini, J. L.; Carignano, M. A. *Macromolecules* **1992**, *25*, 1157.
(19) After the completion of this paper we have been aware of the recent work of E. B. Zhulina and O. V. Borisov (*J. Colloid Interface Sci.* **1990**, *144*, 507), where somewhat similar ideas are discussed. These authors, however, have not considered the present case of star polymers dissolved in a solvent of high molecular weight.
(20) Recent reviews of this work can be found in: Halperin, A; Tirrell, M.; Lodge, T. P. *Adv. Polym. Sci.* **1991**, *100*, 31. Milner, S. T. *Science* **1991**, *251*, 905.
(21) Alexander, S. *J. Phys. (Paris)* **1977**, *38*, 977.
(22) de Gennes, P.-G. *J. Phys. (Paris)* **1976**, *37*, 1443; *Macromolecules* **1980**, *13*, 1069.
(23) Murat, M.; Grest, G. S. *Phys. Rev. Lett.* **1989**, *63*, 1074; *Macromolecules* **1989**, *22*, 4054; *Macromolecules* **1991**, *24*, 704.
(24) Lai, P.-Y.; Binder, K. *J. Chem. Phys.* **1991**, *95*, 9299.
(25) Hirz, S. J. Modeling of Interactions Between Adsorbed Block Copolymer. M.S. Thesis, University of Minnesota, Minneapolis, MN, 1988.
(26) Milner, S. T.; Witten, T. A.; Cates, M. E. *Europhys. Lett.* **1988**, *5*, 413.
(27) Milner, S. T.; Witten, T. A.; Cates, M. E. *Macromolecules* **1988**, *21*, 2610.
(28) Zhulina, E. B.; Pryamitsyn, V. A.; Borisov, O. V. *Vysokomol. Soedin., Ser. A* **1989**, *31*, 185. Zhulina, E. B.; Borisov, O. V.; Pyramitsyn, V. A. *J. Colloid Interface Sci.* **1990**, *137*, 495.
(29) Auroy, P.; Mir, Y.; Auvray, L. *Phys. Rev. Lett.* **1992**, *69*, 93.
(30) Halperin, A. *J. Phys. (Paris)* **1988**, *49*, 547.
(31) Zhulina, E. B.; Borisov, O. V.; Pryamitsyn, V. A.; Birshtein, T. M. *Macromolecules* **1991**, *24*, 140.
(32) de Gennes, P.-G. *Macromolecules* **1980**, *13*, 1069.
(33) See also: Leibler, L. *Makromol. Chem., Macromol. Symp.* **1988**, *16*, 1.
(34) The more delicate problem of a polymer brush exposed to a melt of chemically incompatible polymers has been recently analyzed by E. B. Zhulina and O. V. Borisov by means of self-consistent-field methods (*J. Colloid Interface Sci.* **1990**, *144*, 507).
(35) Pincus, P. *Macromolecules* **1991**, *24*, 2912.
(36) Shim, D. F.; Cates, M. E. *J. Phys. (Paris)* **1989**, *50*, 3535.
(37) These cylindrical blobs are similar to those introduced by F. Brochard-Wyart and E. Raphaël in their studies of molten polymers in small pores (*Macromolecules* **1990**, *23*, 2276).
(38) This problem is similar to the one considered by T. A. Witten and P. Pincus in the context of colloid stabilization by long grafted polymers (*Macromolecules* **1986**, *19*, 2509).
(39) See: Pincus, P. *Macromolecules* **1991**, *24*, 2912.
(40) Joanny, J. F.; Grant, P.; Turkevith, L. A.; Pincus, P. *J. Phys. (Paris)* **1981**, *42*, 1045.
(41) Witten, T. A.; Pincus, P.; Cates, M. E. *Europhys. Lett.* **1986**, *2*, 137.
(42) Flory, P. J. *J. Chem. Phys.* **1949**, *17*, 303.
(43) Edwards, S. F. *Proc. Phys. Soc.* **1969**, *88*, 265.
(44) Flory, P. J. *Principles of Polymer Chemistry*; Cornell University Press: Ithaca, NY, 1971; Chapter XII. Huggins, M. J. *J. Am. Chem. Soc.* **1942**, *64*, 1972.
(45) Note that this analogy for the isolated chain (dilute regime) is also valid in the semidilute and the concentrated regimes. Compare: Daoud, M.; et al. *Macromolecules* **1975**, *8*, 804. Joanny, J. F.; et al. *J. Phys. (Paris)* **1981**, *42*, 1045.